

A GEOMETRICAL NON-LINEAR MODEL FOR CABLE SYSTEMS ANALYSIS

H. Varum ^{*,1}, R.J.S. Cardoso ^{*,2}

^{*}Department of Civil Engineering
University of Aveiro
3810-193, Aveiro, Portugal
E-mail: ¹hvarum@civil.ua.pt, ²rcardoso@civil.ua.pt

Key words: Cables, Non-linear FEA, Green strain, Catenary shape.

Abstract. Cable structures are commonly studied with simplified analytical equations. The evaluation of the accuracy of these equations, in terms of equilibrium geometry configuration and stress distribution was performed for standard cables examples. A three-dimensional finite element analysis (hereafter FEA) procedure based on geometry-dependent stiffness coefficients was developed. The FEA follows a classical procedure in finite element programs, which uses an iterative algorithm, in terms of displacements. The theory is based on a total Lagrange formulation using Green-Lagrange strain. Pure Newton-Raphson procedure was employed to solve the non-linear equations. The results show that the rigid character of the catenary's analytical equation, introduce errors when compared with the FEA.

1 INTRODUCTION

Cables are widely used in suspended bridges, transmission lines or membrane panels [5]. These structural elements are used to transmit tensile forces along a specified curve. Cables can be divided in three categories, in accordance with the acting force field:

- a) Concentrated loads acting on the cable, Fig. 1-a).
- b) Uniformly distributed load acting along a horizontal line, Fig. 1-b).
- c) Uniformly distributed load acting along the cable (corresponding to its self-weight, per example), Fig. 1-c).

For the design of this type of structural elements two approaches are commonly used. The first one corresponds to the use of analytical equations, based on force equilibrium conditions. The second approach consists in the use on numerical finite element models, based on the field displacement of the nodes.

The main issue of this study was to compare results of a non-linear FEA and the analytical equations. In fact, usually when the major action is the self-weight of the cable, catenary's equations are used. The first and second categories of cables were not analyzed in this study.

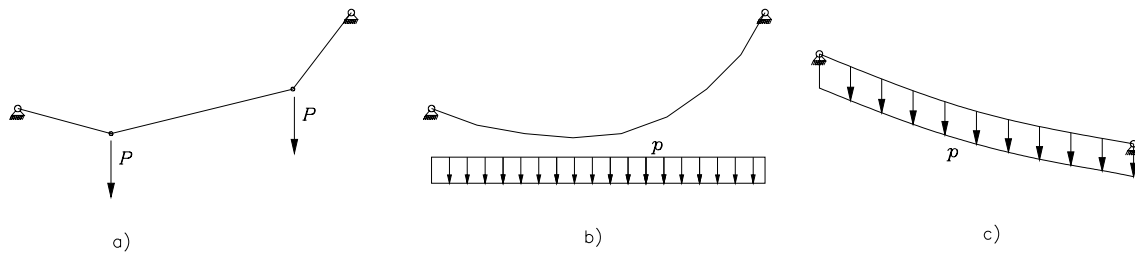


Fig. 1- Cable structures.

2 ANALYTICAL EQUATIONS

As already stated, the determination of the axial force field and geometry configuration of cable structures are usually performed using analytical equations [5]. Catenary's equation is used when load is its self-weight. In the following, the analytical equations of the catenary are introduced (see Fig. 2).

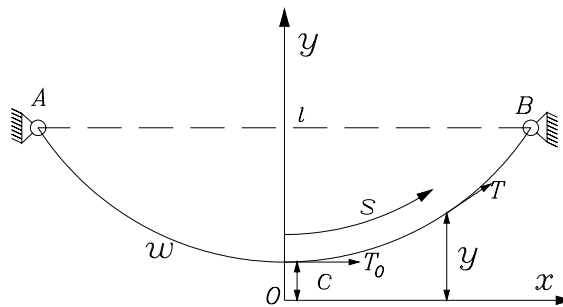


Fig. 2- Catenary's equilibrium configuration.

By the equilibrium conditions, the following equations can be found in [5]:

$$s = c \operatorname{senh} \frac{x}{c} \tag{1}$$

$$y = c \cosh \frac{x}{c} \tag{2}$$

with,

$$T_0 = wc \text{ and } T = wy \tag{3}$$

where,

- s coordinate along the cable,
- x, y coordinates,
- c curve constant parameter,
- w cable self-weight, per unit's length,
- T_0 horizontal axial force at catenary's vertice,
- T axial force for a given y value,
- l span length.

For a given value of s and from Eqs. (1) and (3), the deformed configuration and axial force distribution can be calculated.

3 FEA FORMULATION

3.1 Finite element mesh discretization

In order to analyze and compare the results given by the analytical equations, a series of non-linear FEA were performed. The cable structure adopted in this study is conceived of a continuous series of discrete elements connected to one other by hinged connection. The structure is discretized in n elements and $n + 1$ nodes, as shown in Fig. 3 [4, 8, 9, 11].

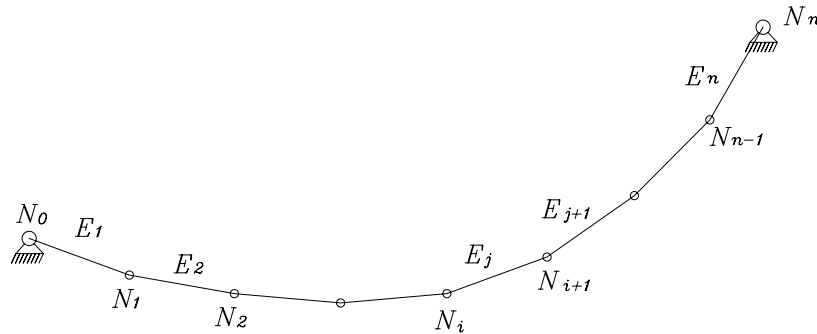


Fig. 3- Cable discretization (nodes and elements).

3.2 Basic element description

The basic element used to describe a cable structure acted by nodal forces submit to large displacements is represented in Fig. 4. The element has two extremity nodes and three independent orthogonal displacements at each node [1, 2, 8, 9, 11].

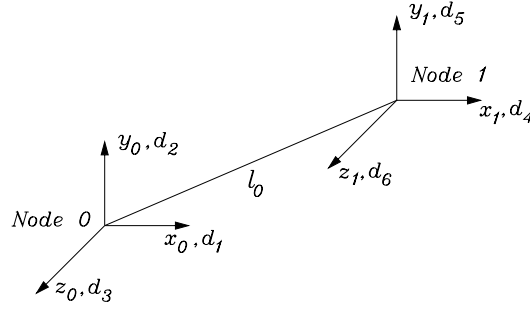


Fig. 4- Basic element.

Length l_0 denotes the initial element length, which define the initial configuration. The initial length is calculated with the nodal coordinates

$$l_0 = \sqrt{(x_1 - x_0)^2 + (y_1 - y_0)^2 + (z_1 - z_0)^2} \quad (4)$$

where x_0, y_0, z_0, x_1, y_1 and z_1 are the nodal coordinates.

The nodal displacements associated with the element $\mathcal{C}^e = \{d_1, d_2, d_3, \dots, d_6\}$, represented in Fig. 4, define the displacement vector per element, and its components are the three independent displacements in each node. The displacement vector of the structure, with the initial configuration allows the definition of the deformed cable and the calculation of the length of each element after deformation.

The length l denotes the length of the element in a deformed configuration,

$$l = \sqrt{(x_1 + d_1 - x_0 - d_4)^2 + (y_1 + d_2 - y_0 - d_5)^2 + (z_1 + d_3 - z_0 - d_6)^2} . \quad (5)$$

Expressions (6), defines the direction of each element in a deformed configuration,

$$\begin{aligned} \cos \alpha_1 &= \frac{x_1 + d_1 - x_0 - d_4}{l} = \frac{l_x}{l}, \quad \cos \alpha_2 = \frac{y_1 + d_2 - y_0 - d_5}{l} = \frac{l_y}{l}, \\ \cos \alpha_3 &= \frac{z_1 + d_3 - z_0 - d_6}{l} = \frac{l_z}{l} \end{aligned} \quad (6)$$

where l_x, l_y and l_z define the projections of the length l on the three orthogonal axes.

3.3 Equilibrium conditions

Eq. (7) establishes the equilibrium conditions along the three orthogonal directions at each node of the cable structure. The incremental displacement vector is the variable to be calculated. Since the occurrence of large displacements was considered, the geometry is non-constant. Thus, stiffness coefficient and internal forces become geometry dependent, and are function of a deformed configuration.

$$K \Delta d = \mathbf{f}_{ext} - \mathbf{f}_{int}, \quad (7)$$

where

- K tangential stiffness matrix obtained assembling the stiffness contribution of all the elements,
- Δd incremental displacement vector,
- \mathbf{f}_{ext} external forces vector (constant),
- \mathbf{f}_{int} internal forces vector.

The problem is solved, in an iterative scheme. When the convergence is reached, the deformed configuration is calculated, and the nodal forces are equilibrated.

The expressions of the tangential stiffness matrix and internal force vector can be found in Varum and Cardoso [8, 9].

3.3.1 Constitutive law and strain

The constitutive law assumed in the implemented model is linear elastic (Hooke's law), expressed by the following expression [3, 7].

$$\sigma = E\varepsilon \quad (8)$$

Since the problem involves large displacements, a total Lagrange formulation is employed in the theory [10], the stiffness coefficients and internal forces were calculated using Green-Lagrange strain definition [1, 6, 11].

$$\varepsilon = \frac{1}{2} \frac{l^2 - l_0^2}{l_0^2}. \quad (9)$$

4 ITERATIVE PROCEDURE

4.1 Newton-Raphson method

The iterative procedure implemented to solve Eq. (10) is based on the Pure Newton-Raphson iterative scheme [3, 7]. To start with the computation, initial stiffness and internal forces are required. Thus initial values are needed for the displacement vector, which is accomplished defining an initial geometry and a deformed geometry.

Assuming static conditions and linear elasticity, the following equation yields for all the nodes.

$$K_i \Delta d_i = f_{ext,i} - f_{int,i} \quad (10)$$

Eq. (10) is solved and the incremental displacement vector Δd is computed. A new displacement vector is obtained with the following equation

$$d_{i+1} = d_i + \Delta d_i \quad (11)$$

This new displacement vector together with the initial constant geometry vector, defines the deformed configuration used in the next step.

As usual, in Pure Newton-Raphson method [2, 3, 7, 11] the better is the estimation of the displacement vector, the faster will be the convergence to the final solution.

4.2 Computational implementation

As already mentioned, the computational implementation of the numerical tool described before follows a classical pattern in finite element programs and use an iterative description of the finite element method. Computations are started given an initial configuration, an initial strain vector and a set of parameters, in order to compute a strain vector increment. The initial configuration vector together with the new strain vector defines a deformed configuration to be used in the next iteration.

The computation procedure is summarised in the following steps:

1. An initial cable's configuration is imposed, namely a constant radius arc defines the nodes position and therefore initial length's cable.
2. An initial strain vector is defined, considering an arc with a slightly larger radius.
3. Initial tangential stiffness and internal forces are computed.
4. Eq. (7) is evaluated and vector Δd is computed.
5. The new strain vector is computed using Eq. (11).
6. Step 2 is repeated until converge is achieved.

5 NUMERICAL EXAMPLES

The numerical examples selected for this study were established in order to compare the results of a geometric non-linear FEA and the analytical equation.

In all the analyses, it was adopted a cable spanning between two rigid end supports that dist 200 m along an horizontal line, the cable initial geometry is a constant radius arc, Fig 5. A longitudinal elastic modulus of $E=200$ GPa, was considered. In both examples, the structures were discretized in 20 elements and 21 nodes.

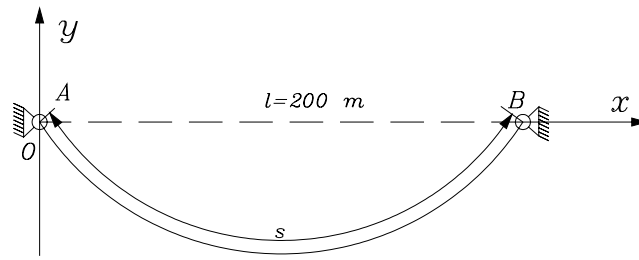


Fig. 5- Cable geometry adopted in the numerical examples.

5.1 Catenary's equation versus FEA

In the set of numerical analyses, the cable in the conditions described in Fig. 5, is subjected to the load corresponding to the self-weight of $w = 0.1 \text{ kN/m}$. The area of the cable is constant and equal to $\Omega = 3.14 \text{ cm}^2$.

Figs. 6, 7, 8 and 9 show the different cable configurations and stress distributions along the cable, obtained in the FEA and with catenary's equation, for four different length's cable.

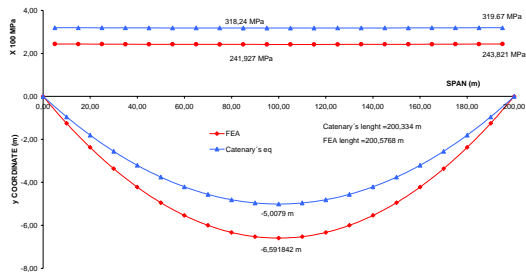


Fig. 6- Cable stress distribution and deformed configuration, $s = 200.3340 \text{ m}$.

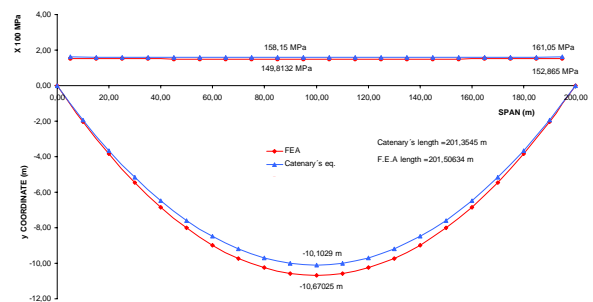


Fig. 7- Cable stress distribution and deformed configuration, $s = 201.3545 \text{ m}$.

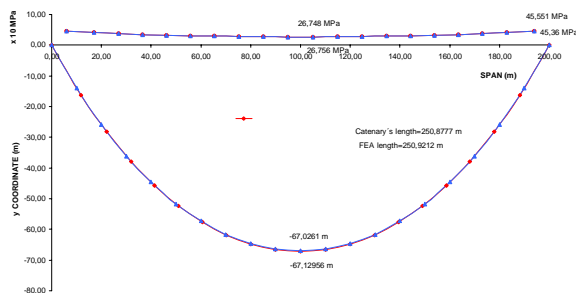


Fig. 8- Cable stress distribution and deformed configuration, $s = 250.8777 \text{ m}$.

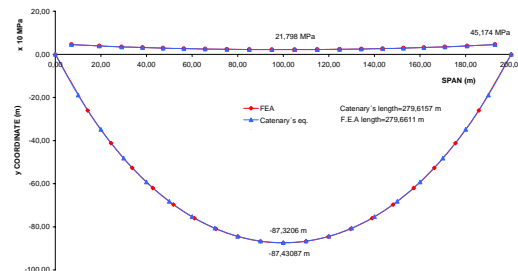


Fig. 9- Cable stress distribution and deformed configuration, $s = 279.6157 \text{ m}$.

From Figs. 6, 7, 8 and 9, it can be observed that the smaller is the initial length of the cable, higher is the stress level. The differences in the deformed configuration and stress level obtain by FEA and Catenary's equation also depends on the cable length or stress level. Figs. 10, 11 and 12 illustrate the differences obtained in maximum stress, minimum stress and maximum y coordinate, using the FEA and Catenary's equation.

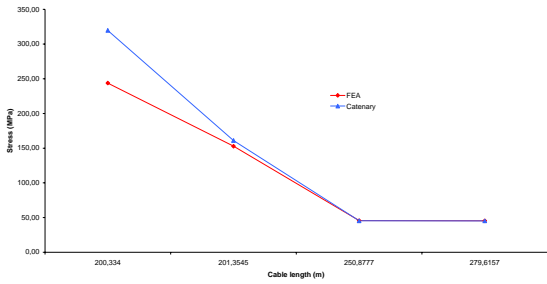


Fig. 10- Maximum cable stress in the support.

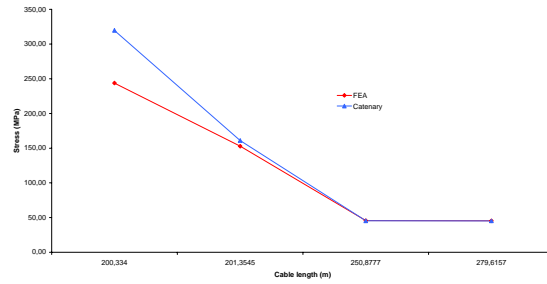


Fig. 11- Minimum cable stress at the vertice.

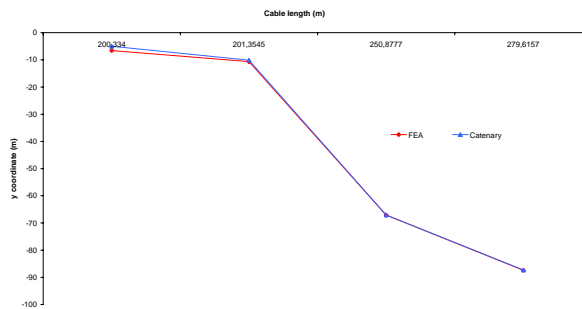


Fig. 12- Maximum y coordinate at mid-span.

6 CONCLUDING REMARKS

In this research, the theoretical formulation, finite element implementation and numerical validation of cable structure are presented to compare FEA and analytical equations results.

The results obtained from the analyses, shows that the solution of a non-linear finite element program are quite different from those given by the analytical expressions.

The analytical expressions are based on a rigid deformed configuration, being the stress distribution and cable geometry a function of it.

When comparing the FEA results with catenary's equation, it was concluded that the length of the cable controls the stress level. The stress level is responsible for a subsequent elastic deformation. Results from the FEA and analytical expressions are approximately equal, when

the maximum stress in the cable is less than 50 MPa, being the error less than 1%. For maximum stress levels of 150 MPa, or higher, the error is approximately 6% and easily reach 30 % (300 MPa).

Finally, it is remarked that geometric non-linear analysis becomes necessary in the studies of cable structures, especially for medium/high stress levels.

ACKNOWLEDGMENTS

The authors would like to thanks the precious help of Professor Victor Dias da Silva, from University of Coimbra, in Portugal, for the theoretical developments included in this article.

REFERENCES

- [1] J.H. ARGYRIS, [et al.], ‘Geometric Nonlinearity and the Finite Element Displacement Method’, in *ISD Lectures on Numerical Methods in Linear and Nonlinear Mechanics*, Jablona 22-28 September 1974. ISD Report N. ° 174 Stuttgart, (1974).
- [2] J.H. ARGYRIS, I. DOLTSINIS, V.D. SILVA, ‘Constitutive Modelling and Computation of Non-Linear Viscoelastic Solids – Part I: Rheological Models and Numerical Integration Techniques’, in *Computers Methods in Applied Mechanics and Engineering*, Vol. 88, N° 2, (1991).
- [3] R.J.S. CARDOSO, ‘Regularização Visco-elástica de Problemas Elasto-plásticos com Amaciamento’, M.Sc Thesis, FCTUC, University of Coimbra (in Portuguese), (2001).
- [4] M.A. CRISFIELD, *Non-linear Finite Element Analysis of Solids and Structures*. Volume 1, Essentials, John Wiley & Sons, (1991).
- [5] D.L. SCHODEK, *Structures*, Fourth Edition, Prentice Hall, Inc., Upper Saddle River, New Jersey (2001).
- [6] V.D. SILVA, *Mecânica e Resistência dos Materiais*, 3ª edição, 452 pags., edição do autor, Coimbra ISBN: 972-98155-1-8, (2004).
- [7] H. VARUM, ‘Modelo Numérico para a Análise Sísmica de Pórticos Planos de Betão Armado,’ M.Sc Thesis, FEUP, University of Porto (in Portuguese), (1995).
- [8] H. VARUM, R.J.S. CARDOSO ‘Finite element simulation of cables behaviour versus analytical equations’ submitted to *Finite Element Analysis and Design*, (2005).
- [9] H. VARUM, R.J.S. CARDOSO ‘Modelo não linear geométrico para a análise de estruturas de cabos’ submitted to *Revista Portuguesa de Engenharia de Estruturas*, Portugal, (2005).
- [10] W. ZHANG, J.L. LEONARD, M.L. ACCORSI, ‘Analysis of geometrically nonlinear anisotropic membranes: theory and verification’, *Finite Elements in Analysis and Design* 41,963-988, (2005).
- [11] O.C. ZIENKIEWICZ, R.L. Taylor, *The Finite Element Method*, MacGraw-Hill, Vol. 2, Fourth Edition, (1989).